Electronic Supplementary Material (ESI) for Journal of Materials Chemistry A.

Supporting Information

Synthesis, Structure and Diffusion Pathways of Fast Lithium-Ion Conductors in the Polymorphs α- and β-Li_8SnP_4

Stefan Strangmüller, Henrik Eickhoff, Wilhelm Klein, Gabriele Raudaschl-Sieber, Holger Kirchhain, Tobias Kutsch, Volodymyr Baran, Anatoliy Senyshyn, Leo van Wüllen, Hubert A. Gasteiger, and Thomas F. Fässler*

Content

Details of the Crystal Structure Determination of α- and β-Li_8SnP_4

Results of the crystal structure determination of α- and β-Li_8SnP_4 from powder neutron diffraction data at low temperatures

Table S1. Atomic coordinates and isotropic atomic displacement parameters of α-Li_8SnP_4 at 4 K.

Atom	Wyckoff positions	*X*	*y*	*z*	U_{eq} / Å^2
Sn	8*c*	0.1264(5)	0.1264(5)	0.1264(5)	0.0188(4)
P1	8*c*	0.2479(4)	0.2479(4)	0.2479(4)	0.022(2)
P2	24*d*	0.0047(4)	0.2526(2)	0.0083(2)	0.0180(7)
Li1	8*c*	0.373(2)	0.373(2)	0.373(2)	0.041(2)
Li2	24*d*	0.3834(9)	0.132(1)	0.137(1)	0.022(2)
Li3	24*d*	0.376(2)	0.372(1)	0.120(1)	0.033(1)
Li4	4*a*	0	0	0	0.16(1)
Li5	4*b*	½	1/2	1/2	0.093(6)

Table S2. Selected interatomic distances in α-Li_8SnP_4 at 4 K.

Atom pair			d / Å	Atom pair			d / Å
Sn	P1	1×	2.511(8)	Li2	P1	1×	2.51(1)
	P2	3×	2.523(7)		P2	1×	2.64(1)
	Li5	1×	2.612(6)		Li4	1×	2.66(1)
	Li3	3×	3.04(2)		P2	1×	2.66(1)
	Li2	3×	3.07(1)		Li3	1×	2.86(2)
P1	Li2	3×	2.51(1)		Li3	1×	2.87(2)
	Sn	1×	2.511(8)		Li2	2×	2.98(2)
	Li1	1×	2.58(2)		Sn	1×	3.07(1)
	Li3	3×	2.61(2)		Li1	1×	3.15(2)
P2	Li2	1×	2.51(1)	Li3	Li5	1×	2.57(2)
	Sn	1×	2.523(7)		P1	1×	2.61(2)
	Li1	1×	2.56(2)		P2	1×	2.62(2)
	Li3	1×	2.62(2)		P2	1×	2.63(2)
	Li3	1×	2.63(2)		P2	1×	2.64(2)
	Li3	1×	2.64(2)		Li2	1×	2.86(3)
	Li2	1×	2.64(1)		Li2	1×	2.87(2)
	Li2	1×	2.66(1)		Li3	2×	2.92(3)
	Li4	1×	2.954(2)		Li1	1×	3.02(3)
	Li5	1×	3.016(2)		Sn	1×	3.04(2)
Li1	P2	3×	2.56(2)	Li4	Li1	2×	2.63(2)
	P1	1×	2.58(2)		Li2	6×	2.66(1)
	Li4	1×	2.63(2)		P2	6×	2.954(5)
	Li3	3×	3.02(3)	Li5	Li3	6×	2.57(2)
	Li2	3×	3.15(2)		Sn	2×	2.612(6)
Li2	P2	1×	2.51(1)		P2	6×	3.016(2)

Table S3. Bond angles of SnP_4 and LiP_4 tetrahedra in α-Li_8SnP_4 at 4 K.

Atom 1 − 2 − 3	Angle / deg	Atom 1 − 2 − 3	Angle / deg
P1 − Sn − P2	108.1(3)	P2 − Sn − P2	110.8(2)
P1 − Sn − P2	108.1(3)	P2 − Sn − P2	110.8(2)
P1 − Sn − P2	108.1(3)	P2 − Sn − P2	110.8(2)
P2 − Li1 − P2	108.4(8)	P1 − Li1 − P2	110.5(8)
P2 − Li1 − P2	108.4(8)	P1 − Li1 − P2	110.5(8)
P2 − Li1 − P2	108.4(8)	P1 − Li1 − P2	110.5(8)
P2 − Li2 − P2	102.9(4)	P1 − Li2 − P2	103.9(4)
P2 − Li2 − P2	108.9(4)	P1 − Li2 − P2	114.4(4)
P2 − Li2 − P2	109.6(4)	P1 − Li2 − P2	116.0(5)
P2 − Li3 − P2	104.3(6)	P1 − Li3 − P2	107.2(6)
P2 − Li3 − P2	112.4(5)	P1 − Li3 − P2	108.5(5)
P2 − Li3 − P2	112.8(6)	P1 − Li3 − P2	111.3(7)

Table S4. Bond angles of LiP_6 octahedra in α-Li_8SnP_4 at 4 K.

Atom 1 − 2 − 3	Angle / deg	Atom 1 − 2 − 3	Angle / deg
P2 − Li4 − P2	89.2(1)	P2 − Li5 − P2	87.0(1)
P2 − Li4 − P2	89.2(1)	P2 − Li5 − P2	87.0(1)
P2 − Li4 − P2	89.2(1)	P2 − Li5 − P2	87.0(1)
P2 − Li4 − P2	89.2(1)	P2 − Li5 − P2	87.0(1)
P2 − Li4 − P2	89.21(6)	P2 − Li5 − P2	87.03(6)
P2 − Li4 − P2	89.21(6)	P2 − Li5 − P2	87.03(6)
P2 − Li4 − P2	90.8(1)	P2 − Li5 − P2	93.0(1)
P2 − Li4 − P2	90.8(1)	P2 − Li5 − P2	93.0(1)
P2 − Li4 − P2	90.8(1)	P2 − Li5 − P2	93.0(1)
P2 − Li4 − P2	90.8(1)	P2 − Li5 − P2	93.0(1)
P2 − Li4 − P2	90.79(6)	P2 − Li5 − P2	93.0(6)
P2 − Li4 − P2	90.79(6)	P2 − Li5 − P2	93.0(6)
P2 − Li4 − P2	180	P2 − Li5 − P2	180
P2 − Li4 − P2	180	P2 − Li5 − P2	180
P2 − Li4 − P2	180	P2 − Li5 − P2	180

Table S5. Atomic coordinates and isotropic atomic displacement parameters of β-Li_8SnP_4 at 10 K.

Atom	Wyckoff positions	*x*	*y*	*z*	s.o.f.	U_{eq} / Å^2
Sn1	2*a*	1/2	1/2	1/2	---	0.023(2)
P1	8*e*	0.3784(5)	0.3784(5)	0.3784(5)	---	0.024(3)
Sn2	6*c*	1/4	1/2	0	---	0.0208(8)
P2	24*i*	0.1309(3)	0.3804(4)	0.1250(3)	---	0.026(1)
Li1	6*b*	0	1/2	0	---	0.023(5)
Li2	6*d*	0	1/2	1/4	---	0.047(5)
Li3	8*e*	0.248(2)	0.248(2)	0.248(2)	---	0.056(9)
Li4	12*f*	0	0.250(1)	0	---	0.038(4)
Li5	24*i*	0.2405(7)	0.2425(7)	0.005(1)	---	0.024(2)
Li6	8*e*	0.139(3)	0.139(3)	0.139(3)	0.5(1)	0.07(2)
Li7	24*i*	0.39(1)	0.36(1)	0.10(1)	0.16(4)	0.14(4)

Table S6. Selected interatomic distances in β-Li_8SnP_4 at 10 K.

Atom pair			d / Å	Atom pair			d / Å	Atom pair			d / Å
Sn1	P1	4×	2.515(6)	Li1	P2	4×	2.591(4)	Li5	P2	1×	2.66(1)
	Li6	4×	2.88(4)		Li4	2×	2.98(2)		Li4	1×	2.874(8)
	Li4	6×	2.99(2)		Sn2	2×	2.986(1)		Li4	1×	2.90(2)
P1	Sn1	1×	2.515(6)		Li2	2×	2.986(1)		Li3	1×	2.90(3)
	Li5	3×	2.53(1)	Li2	Li7	4×	2.2(1)		Li7	1×	3.0(1)
	Li4	3×	2.57(1)		P2	4×	2.591(4)		Li3	1×	3.08(3)
	Li3	1×	2.70(2)		Li1	2×	2.986(1)		Sn2	1×	3.078(8)
	Li6	3×	3.13(4)		Li5	4×	3.101(8)		Li2	1×	3.101(8)
	Li7	3×	3.3(1)	Li3	Li6	1×	2.25(4)	Li6	Li3	1×	2.25(4)
Sn2	P2	4×	2.508(4)		P2	3×	2.57(2)		Li5	3×	2.36(4)
	Li7	4×	2.7(1)		P1	1×	2.70(2)		Li4	3×	2.70(4)
	Li1	2×	2.986(1)		Li7	3×	2.7(1)		Sn1	1×	2.88(4)
	Li5	4×	3.08(2)		Li5	3×	2.90(3)		P2	3×	2.89(4)
P2	Sn2	1×	2.508(4)		Li5	3×	3.08(3)		P1	3×	3.13(4)
	Li5	1×	2.54(1)	Li4	P1	2×	2.57(1)	Li7	Li2	1×	2.2(1)
	Li3	1×	2.57(2)		P2	2×	2.66(1)		Li1	1×	2.5(1)
	Li1	1×	2.591(4)		Li6	2×	2.70(4)		Li5	1×	2.5(1)
	Li2	1×	2.591(4)		Li7	2×	2.8(2)		Li5	1×	2.6(1)
	Li5	1×	2.65(1)		Li5	2×	2.874(8)		Sn2	1×	2.7(1)
	Li4	1×	2.66(1)		Li5	2×	2.90(2)		P2	1×	2.7(2)
	Li5	1×	2.66(1)		Li1	1×	2.98(2)		Li3	1×	2.7(1)
	Li7	1×	2.7(2)		Sn1	1×	2.99(2)		Li4	1×	2.8(2)
	Li7	1×	2.8(2)	Li5	Li6	1×	2.36(4)		P2	1×	2.8(2)
	Li6	1×	2.89(4)		Li7	1×	2.5(1)		P2	1×	2.9(1)
	Li7	1×	2.9(1)		P1	1×	2.53(1)		Li5	1×	3.0(1)
	Li7	1×	3.1(1)		P2	1×	2.54(1)		P2	1×	3.1(1)
	Li7	1×	3.2(2)		Li7	1×	2.6(1)		P2	1×	3.2(2)
Li1	Li7	4×	2.5(1)		P2	1×	2.65(1)		P1	1×	3.3(2)

Table S7. Bond angles of SnP_4 and LiP_4 tetrahedra in β-Li_8SnP_4 at 10 K.

Atom 1 − 2 − 3				Angle / deg	Atom 1 − 2 − 3				Angle / deg
P1	−	Sn1	− P1	109.47	P1	−	Sn1	− P1	109.47
P1	−	Sn1	− P1	109.47	P1	−	Sn1	− P1	109.47
P1	−	Sn1	− P1	109.47	P1	−	Sn1	− P1	109.47
P2	−	Sn2	− P2	108.8(1)	P2	−	Sn2	− P2	108.8(1)
P2	−	Sn2	− P2	108.8(1)	P2	−	Sn2	− P2	110.9(1)
P2	−	Sn2	− P2	108.8(1)	P2	−	Sn2	− P2	110.9(1)
P2	−	Li1	− P2	105.8(1)	P1	−	Li1	− P2	109.6(1)
P2	−	Li1	− P2	105.8(1)	P1	−	Li1	− P2	113.1(1)
P2	−	Li1	− P2	109.6(1)	P1	−	Li1	− P2	113.1(1)
P2	−	Li2	− P2	109.4(1)	P2	−	Li2	− P2	109.4(1)
P2	−	Li2	− P2	109.4(1)	P2	−	Li2	− P2	109.6(1)
P2	−	Li2	− P2	109.4(1)	P2	−	Li2	− P2	109.6(1)
P1	−	Li3	− P2	106.8(8)	P2	−	Li3	− P2	112.0(9)
P1	−	Li3	− P2	106.8(8)	P2	−	Li3	− P2	112.0(9)
P1	−	Li3	− P2	106.8(8)	P2	−	Li3	− P2	112.0(9)
P1	−	Li4	− P1	106.3(2)	P1	−	Li4	− P2	109.6(2)
P2	−	Li4	− P2	108.6(1)	P1	−	Li4	− P2	111.3(2)
P1	−	Li4	− P2	109.6(2)	P1	−	Li4	− P2	111.4(2)
P2	−	Li5	− P2	103.1(4)	P2	−	Li5	− P2	110.4(3)
P2	−	Li5	− P2	105.6(4)	P1	−	Li5	− P2	113.0(4)
P1	−	Li5	− P2	109.2(3)	P1	−	Li5	− P2	114.7(4)

Table S8. Bond angles of LiP_6 octahedra in β-Li_8SnP_4 at 10 K.

Atom 1 − 2 − 3					Angle / deg	Atom 1 − 2 − 3					Angle / deg
P1	−	Li6	−	P1	82.1(9)	P2	−	Li7	−	P2	81(3)
P1	−	Li6	−	P1	82.1(9)	P2	−	Li7	−	P1	82(4)
P1	−	Li6	−	P1	82.1(9)	P2	−	Li7	−	P1	83(3)
P2	−	Li6	−	P1	90(1)	P2	−	Li7	−	P1	87(4)
P2	−	Li6	−	P1	90(1)	P2	−	Li7	−	P1	88(4)
P2	−	Li6	−	P1	90(1)	P2	−	Li7	−	P2	89(4)
P2	−	Li6	−	P1	91(1)	P2	−	Li7	−	P2	90(4)
P2	−	Li6	−	P1	91(1)	P2	−	Li7	−	P2	90(4)
P2	−	Li6	−	P1	92(1)	P2	−	Li7	−	P2	93(4)
P2	−	Li6	−	P2	95(1)	P2	−	Li7	−	P2	95(4)
P2	−	Li6	−	P2	95(1)	P2	−	Li7	−	P2	98(4)
P2	−	Li6	−	P2	95(1)	P2	−	Li7	−	P2	101(5)
P2	−	Li6	−	P1	171(1)	P2	−	Li7	−	P2	168(5)
P2	−	Li6	−	P1	171(1)	P2	−	Li7	−	P2	168(6)
P2	−	Li6	−	P1	171(1)	P2	−	Li7	−	P1	170(6)

Results of the crystal structure determination of α- and β-Li_8SnP_4 from powder neutron diffraction data at 300 K

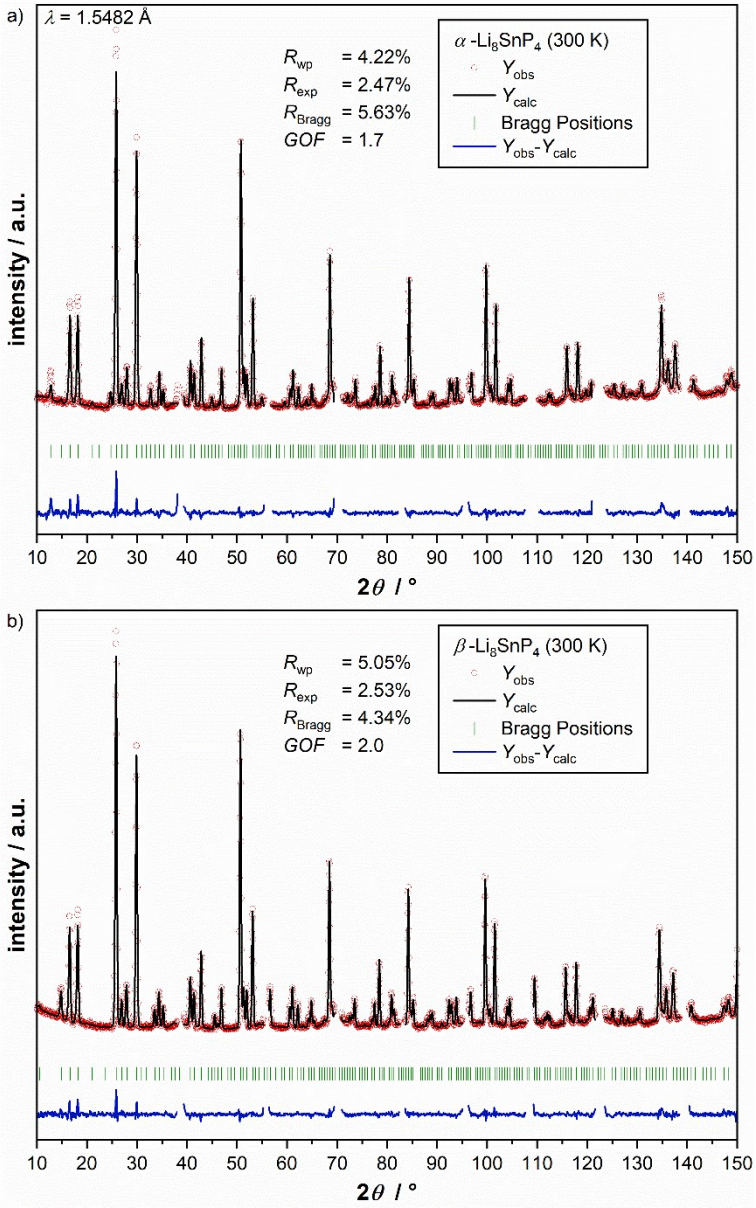

Figure S1. Results from the Rietveld structure refinements of α- and β-Li_8SnP_4 at 300 K. a) Rietveld analysis of the powder neutron diffraction pattern of α-Li_8SnP_4 at 300 K. b) Rietveld analysis of the powder neutron diffraction pattern of β-Li_8SnP_4 at 300 K. In both diffraction patterns red circles indicate observed intensities Y_{obs}, black lines show calculated intensities Y_{calc}, blue lines reveal the difference between observed and calculated intensities, and green marks indicate Bragg positions of the corresponding phase α- and β-Li_8SnP_4. The reflection positions of Nb (ampule) reflection have been excluded from the refinement.

Table S9. Details of the Rietveld structure refinement of α- and β-Li_8SnP_4 at 300 K.

Empirical formula	α-Li_8SnP_4	β-Li_8SnP_4
T / K	300	300
Formula weight / g·mol^{-1}	298.1	298.1
Space group (no.)	$Pa\bar{3}$ (205)	$P\bar{4}3n$ (218)
Unit cell parameters / Å	a = 11.97626(6)	a = 11.99307(6)
Z	8	8
V / Å^3	1717.77(2)	1725.01(2)
$\rho_{calc.}$ / g·cm^{-3}	2.305	2.296
2θ range / deg	10.000-151.000	10.000-151.000
R_p	3.53 %	3.38 %
R_{wp}	4.22 %	5.05 %
R_{exp}	2.47 %	2.53 %
X^2	2.90 %	3.99 %
GOF	1.7	2.0
R_{Bragg}	5.63 %	4.34 %
R_f	6.11 %	4.85 %
Depository no.	CSD-2059625	CSD-2061134

Table S10. Atomic coordinates and isotropic atomic displacement parameters of α-Li_8SnP_4 at 300 K.

Atom	Wyckoff positions	*x*	*y*	*z*	U_{eq} / Å^2
Sn	8*c*	0.1261(4)	0.1261(4)	0.1261(4)	0.0267(5)
P1	8*c*	0.2468(4)	0.2468(4)	0.2468(4)	0.021(1)
P2	24*d*	0.0049(4)	0.2538(2)	0.0082(2)	0.0272(5)
Li1	8*c*	0.3819(18)	0.382(2)	0.382(2)	0.054(5)
Li2	24*d*	0.3863(8)	0.135(1)	0.1333(9)	0.032(1)
Li3	24*d*	0.375(2)	0.372(1)	0.125(1)	0.044(1)
Li4	4*a*	0	0	0	0.18(1)
Li5	4*b*	1/2	1/2	1/2	0.067(4)

Table S11. Atomic coordinates and isotropic atomic displacement parameters of β-Li_8SnP_4 at 300 K.

Atom	Wyckoff positions	*x*	*y*	*z*	s.o.f.	U_{eq} / Å^2
Sn1	2*a*	1/2	1/2	1/2	---	0.030(3)
P1	8*e*	0.3770(5)	0.3770(5)	0.3770(5)	---	0.024(3)
Sn2	6*c*	1/4	1/2	0	---	0.027(1)
P2	24*i*	0.1321(5)	0.3811(5)	0.1238(5)	---	0.030(1)
Li1	6*b*	0	1/2	0	---	0.033(8)
Li2	6*d*	0	1/2	1/4	---	0.064(7)
Li3	8*e*	0.248(3)	0.248(3)	0.248(3)	---	0.05(1)
Li4	12*f*	0	0.249(2)	0	---	0.042(6)
Li5	24*i*	0.242(1)	0.241(1)	0.007(2)	---	0.044(5)
Li6	8*e*	0.142(3)	0.142(3)	0.142(3)	0.7(1)	0.08(1)
Li7	24*i*	0.39(2)	0.37(2)	0.11(2)	0.09(4)	0.08(1)

Results of the crystal structure determination of α- and β-Li_8SnP_4 from powder neutron diffraction data at high temperature

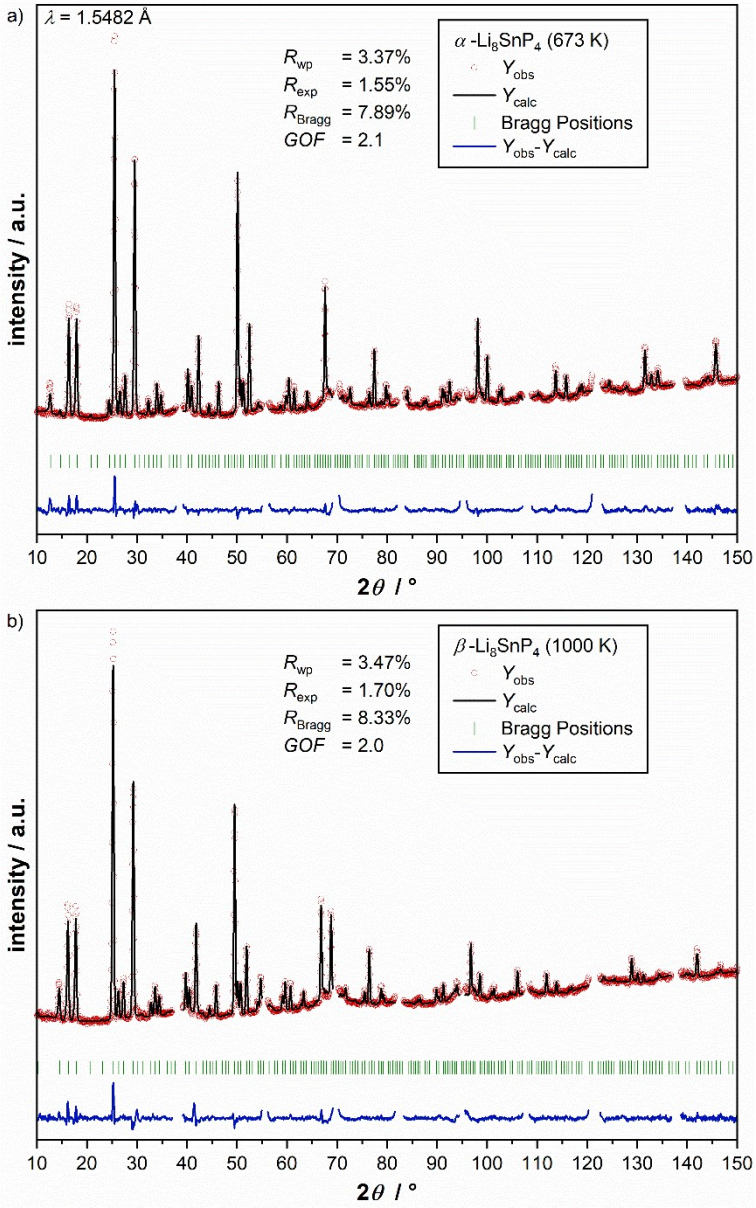

Figure S2. Results from the Rietveld structure refinements of α- and β-Li_8SnP_4 at high temperature. a) Rietveld analysis of the powder neutron diffraction pattern of α-Li_8SnP_4 at 673 K. b) Rietveld analysis of the powder neutron diffraction pattern of β-Li_8SnP_4 at 1000 K. In both diffraction patterns red circles indicate observed intensities Y_{obs}, black lines show calculated intensities Y_{calc}, blue lines reveal the difference between observed and calculated intensities, and green marks indicate Bragg positions of the corresponding phase α- and β-Li_8SnP_4. The reflection positions of Nb (ampule) have been excluded from the refinement.

Table S12. Details of the Rietveld structure refinement of α- and β-Li_8SnP_4 at high temperature.

Empirical formula	α-Li_8SnP_4	β-Li_8SnP_4
T / K	673	1000
Formula weight / g·mol^{-1}	298.1	298.1
Space group (no.)	$Pa\bar{3}$ (205)	$P\bar{4}3n$ (218)
Unit cell parameters / Å	a = 12.12543(9)	a = 12.2564(1)
Z	8	8
V / Å^3	1782.75(2)	1841.14(4)
$\rho_{calc.}$ / g·cm^{-3}	2.221	2.151
2θ range / deg	10.000-151.000	10.000-151.000
R_p	2.62 %	2.54 %
R_{wp}	3.37 %	3.47 %
R_{exp}	1.55 %	1.70 %
X^2	4.71 %	4.20 %
GOF	2.1	2.0
R_{Bragg}	7.89 %	8.33 %
R_f	14.2 %	14.0 %
Depository no.	CSD-2059626	CSD-2061135

Table S13. Atomic coordinates and isotropic atomic displacement parameters of α-Li_8SnP_4 at 673 K.

Atom	Wyckoff positions	*x*	*y*	*z*	U_{eq} / Å^2
Sn	8*c*	0.126(1)	0.126(1)	0.126(1)	0.0432(8)
P1	8*c*	0.2468(5)	0.2468(5)	0.2468(5)	0.035(2)
P2	24*d*	0.0068(6)	0.2507(5)	0.0091(2)	0.0437(8)
Li1	8*c*	0.373(6)	0.373(6)	0.373(6)	0.113(7)
Li2	24*d*	0.379(3)	0.122(5)	0.132(3)	0.076(3)
Li3	24*d*	0.381(4)	0.372(3)	0.121(3)	0.073(3)
Li4	4*a*	0	0	0	0.25(2)
Li5	4*b*	1/2	1/2	1/2	0.104(7)

Table S14. Atomic coordinates and isotropic atomic displacement parameters of β-Li_8SnP_4 at 1000 K.

Atom	Wyckoff positions	*x*	*y*	*z*	s.o.f.	U_{eq} / Å^2
Sn1	2*a*	1/2	1/2	1/2	---	0.078(7)
P1	8*e*	0.3772(6)	0.3772(6)	0.3772(6)	---	0.038(2)
Sn2	6*c*	1/4	1/2	0	---	0.058(3)
P2	24*i*	0.1367(4)	0.3798(7)	0.1215(5)	---	0.060(1)
Li1	6*b*	0	1/2	0	---	0.10(2)
Li2	6*d*	0	1/2	1/4	---	0.16(8)
Li3	8*e*	0.240(2)	0.240(2)	0.240(2)	---	0.060(8)
Li4	12*f*	0	0.239(3)	0	---	0.10(1)
Li5	24*i*	0.231(2)	0.238(1)	0.024(3)	---	0.106(7)
Li6	8*e*	0.144(1)	0.144(1)	0.144(1)	0.45(4)	0.017(7)
Li7	24*i*	0.323(4)	0.383(4)	0.185(4)	0.18(1)	0.017(7)

Results of the crystal structure determination of β-Li_8SnP_4 from single crystal data at 293 K

Table S15. Atomic coordinates of β-Li_8SnP_4 at 293 K.

Atom	Wyckoff positions	*x*	*y*	*z*	s.o.f.
Sn1	2*a*	1/2	1/2	1/2	---
P1	8*e*	0.37861(5)	0.37861(5)	0.37861(5)	---
Sn2	6*c*	1/4	1/2	0	---
P2	24*i*	0.13151(5)	0.38095(5)	0.12603(4)	---
Li1	6*b*	0	1/2	0	0.787(7)
Li2	6*d*	0	1/2	1/4	---
Li3	8*e*	0.2558(4)	0.2558(4)	0.2558(4)	---
Li4	12*f*	0	0.2541(5)	0	---
Li5	24*i*	0.2397(7)	0.2427(5)	0.0028(9)	0.926(2)
Li6	8*e*	0.139(1)	0.139(1)	0.139(1)	0.809(6)
Li7	24*i*	0.404(3)	0.376(2)	0.121(2)	0.191(2)

Table S16. Anisotropic displacement parameters (Å^2) of β-Li_8SnP_4 at 293 K.

Atom	U_{11}	U_{22}	U_{33}	U_{23}	U_{13}	U_{12}
Sn1	0.00957(8)	0.00957(8)	0.00957(8)	0	0	0
P1	0.0109(2)	0.0109(2)	0.0109(2)	−0.0009(1)	−0.0009(1)	−0.0009(1)
Sn2	0.0114(1)	0.01345(7)	0.01345(7)	0	0	0
P2	0.0141(3)	0.0121(3)	0.0139(3)	−0.0010(2)	0.0001(2)	0.0008(2)
Li1	0.03(1)	0.13(2)	0.023(9)	0	0	0
Li2	0.016(2)	0.016(2)	0.007(3)	0	0	0
Li3	0.014(1)	0.014(1)	0.014(1)	−0.005(1)	−0.005(1)	−0.005(1)
Li4	0.013(2)	0.019(3)	0.014(2)	0	−0.001(2)	0
Li5	0.034(3)	0.022(3)	0.046(4)	−0.003(2)	−0.022(5)	−0.002(5)
Li6	0.11(1)	0.11(1)	0.11(1)	−0.027(9)	−0.027(9)	−0.027(9)
Li7	0.11(1)	0.11(1)	0.11(1)	−0.027(9)	−0.027(9)	−0.027(9)

Table S17. Selected interatomic distances in β-Li_8SnP_4 at 293 K.

Atom pair			d / Å	Atom pair			d / Å	Atom pair			d / Å
Sn1	P1	4×	2.5187(6)	Li1	P2	4×	2.6068(6)	Li5	Li7	1×	2.82(3)
	Li6	4×	2.88(2)		Li4	2×	2.946(6)		Li4	1×	2.875(8)
	Li4	6×	3.044(6)		Sn2	2×	2.9948(1)		Li7	1×	2.90(3)
P1	Li5	3×	2.517(9)		Li2	2×	2.9948(1)		Li4	1×	2.913(9)
	Sn1	1×	2.5187(6)	Li2	Li7	4×	2.39(3)		Li3	1×	2.96(1)
	Li3	1×	2.548(5)		P2	4×	2.5925(6)		Li3	1×	3.04(1)
	Li4	3×	2.599(3)		Li1	2×	2.9948(1)		Sn2	1×	3.085(6)
	Li7	3×	3.10(4)		Li5	4×	3.120(8)		Li2	1×	3.120(8)
	Li6	3×	3.13(2)	Li3	Li6	1×	2.43(2)	Li6	Li5	3×	2.38(2)
Sn2	P2	4×	2.5156(6)		P1	1×	2.548(5)		Li3	1×	2.43(2)
	Li7	4×	2.78(3)		P2	3×	2.623(5)		Li4	3×	2.73(2)
	Li1	2×	2.9948(1)		Li7	3×	2.80(3)		Sn1	1×	2.88(2)
	Li5	4×	3.09(1)		Li5	3×	2.96(1)		P2	3×	2.91(2)
P2	Sn2	1×	2.5156(6)		Li5	3×	3.04(1)		P1	3×	3.13(2)
	Li5	1×	2.569(9)	Li4	Li7	2×	2.40(3)	Li7	Li1	1×	2.37(3)
	Li2	1×	2.5925(6)		P1	2×	2.599(4)		Li2	1×	2.39(3)
	Li1	1×	2.6068(6)		P2	2×	2.659(4)		Li4	1×	2.40(3)
	Li3	1×	2.623(5)		Li6	2×	2.73(2)		Li5	1×	2.49(3)
	Li5	1×	2.643(9)		Li5	2×	2.875(8)		P2	1×	2.73(4)
	Li4	1×	2.659(4)		Li5	2×	2.91(1)		Sn2	1×	2.78(3)
	Li5	1×	2.682(8)		Li1	1×	2.946(6)		Li3	1×	2.80(3)
	Li7	1×	2.73(4)		Sn1	1×	3.044(6)		Li5	1×	2.82(3)
	Li6	1×	2.91(2)	Li5	Li6	1×	2.38(2)		Li5	1×	2.90(3)
	Li7	1×	2.91(2)		Li7	1×	2.49(3)		P2	1×	2.91(2)
	Li7	1×	3.01(2)		P1	1×	2.517(9)		P2	1×	3.01(2)
	Li7	1×	3.03(2)		P2	1×	2.569(9)		P2	1×	3.03(2)
	Li7	1×	3.27(4)		P2	1×	2.643(9)		P1	1×	3.10(2)
Li1	Li7	4×	2.37(3)		P2	1×	2.682(9)		P2	1×	3.27(4)

Table S18. Bond angles of SnP_4 and LiP_4 tetrahedra in β-Li_8SnP_4 at 293K.

Atom 1 − 2 − 3					Angle / deg	Atom 1 − 2 − 3					Angle / deg
P1	−	Sn1	−	P1	109.47	P1	−	Sn1	−	P1	109.47
P1	−	Sn1	−	P1	109.47	P1	−	Sn1	−	P1	109.47
P1	−	Sn1	−	P1	109.47	P1	−	Sn1	−	P1	109.47
P2	−	Sn2	−	P2	108.57(2)	P2	−	Sn2	−	P2	108.57(2)
P2	−	Sn2	−	P2	108.57(2)	P2	−	Sn2	−	P2	111.30(2)
P2	−	Sn2	−	P2	108.57(2)	P2	−	Sn2	−	P2	111.30(2)
P2	−	Li1	−	P2	105.64(2)	P1	−	Li1	−	P2	109.22(2)
P2	−	Li1	−	P2	105.64(2)	P1	−	Li1	−	P2	113.66(2)
P2	−	Li1	−	P2	109.22(2)	P1	−	Li1	−	P2	113.66(2)
P2	−	Li2	−	P2	109.16(2)	P2	−	Li2	−	P2	109.16(2)
P2	−	Li2	−	P2	109.16(2)	P2	−	Li2	−	P2	110.11(2)
P2	−	Li2	−	P2	109.16(2)	P2	−	Li2	−	P2	110.11(2)
P2	−	Li3	−	P2	109.1(2)	P1	−	Li3	−	P2	109.9(2)
P2	−	Li3	−	P2	109.1(2)	P1	−	Li3	−	P2	109.9(2)
P2	−	Li3	−	P2	109.1(2)	P1	−	Li3	−	P2	109.9(2)
P1	−	Li4	−	P1	104.59(2)	P2	−	Li4	−	P2	110.29(2)
P1	−	Li4	−	P2	109.62(2)	P1	−	Li4	−	P2	111.31(2)
P1	−	Li4	−	P2	109.62(2)	P1	−	Li4	−	P2	111.31(2)
P2	−	Li5	−	P2	103.2(3)	P1	−	Li5	−	P2	110.2(3)
P2	−	Li5	−	P2	105.0(3)	P1	−	Li5	−	P2	113.2(3)
P2	−	Li5	−	P2	108.9(2)	P1	−	Li5	−	P2	115.3(3)

Table S19. Bond angles of LiP_6 octahedra in β-Li_8SnP_4 at 293K.

Atom 1 − 2 − 3					Angle / deg	Atom 1 − 2 − 3					Angle / deg
P1	−	Li6	−	P1	82.0(4)	P2	−	Li7	−	P2	80.9(7)
P1	−	Li6	−	P1	82.0(4)	P2	−	Li7	−	P2	82.7(7)
P1	−	Li6	−	P1	82.0(4)	P1	−	Li7	−	P2	83.3(7)
P2	−	Li6	−	P1	90.7(5)	P2	−	Li7	−	P2	85.7(7)
P2	−	Li6	−	P1	90.7(5)	P2	−	Li7	−	P1	87.7(6)
P2	−	Li6	−	P1	90.7(5)	P2	−	Li7	−	P2	88.9(6)
P2	−	Li6	−	P1	91.9(5)	P2	−	Li7	−	P1	89.1(6)
P2	−	Li6	−	P1	91.9(5)	P2	−	Li7	−	P2	91.1(7)
P2	−	Li6	−	P1	91.9(5)	P2	−	Li7	−	P2	94.8(8)
P2	−	Li6	−	P2	94.7(5)	P2	−	Li7	−	P1	96.1(8)
P2	−	Li6	−	P2	94.7(5)	P2	−	Li7	−	P2	97.9(9)
P2	−	Li6	−	P2	94.7(5)	P2	−	Li7	−	P2	98.6(9)
P2	−	Li6	−	P1	171.1(6)	P2	−	Li7	−	P1	166.0(9)
P2	−	Li6	−	P1	171.1(6)	P2	−	Li7	−	P2	166.5(9)
P2	−	Li6	−	P1	171.1(6)	P2	−	Li7	−	P2	179(1)

Coordination Polyhedra of *α*-and *β*-Li_8SnP_4

In *α*-Li_8SnP_4 the Sn atom is surrounded by one atom P1 and three atoms P2 in a slightly distorted tetrahedral geometry (Figure S3a). Additionally, one atom Li5 and three unoccupied sites (24*d*) can be found within a radius of about 2.7 Å. The P atoms (P1 and P2) are centered in a slightly distorted cubic geometry consisting of one Sn atom, one Li1 atom, three Li2 atoms, and three Li3 atoms, each (Figures 3b, c).

Regarding the next nearest coordination spheres, the Sn atom is centered in a slightly distorted octahedral geometry generated by six Li atoms (3×Li2 and 3×Li3), whereas the atom P1 is surrounded by six unoccupied positions (24*d*). The octahedra in the vicinity of the atom P2 contains two Li atoms (1×Li4 and 1×Li5) and four unoccupied sites (24*d*, Figures S3d, e, f).

Moreover, the coordination polyhedra of the atoms Li1-Li5 are depicted (Figure S4) as they reveal the connection of occupied and unoccupied tetrahedral and octahedral voids, which is essential for the understanding of the diffusion pathways (one-particle potential) based on nuclear density maps obtained by powder neutron diffraction experiments at 673 K.

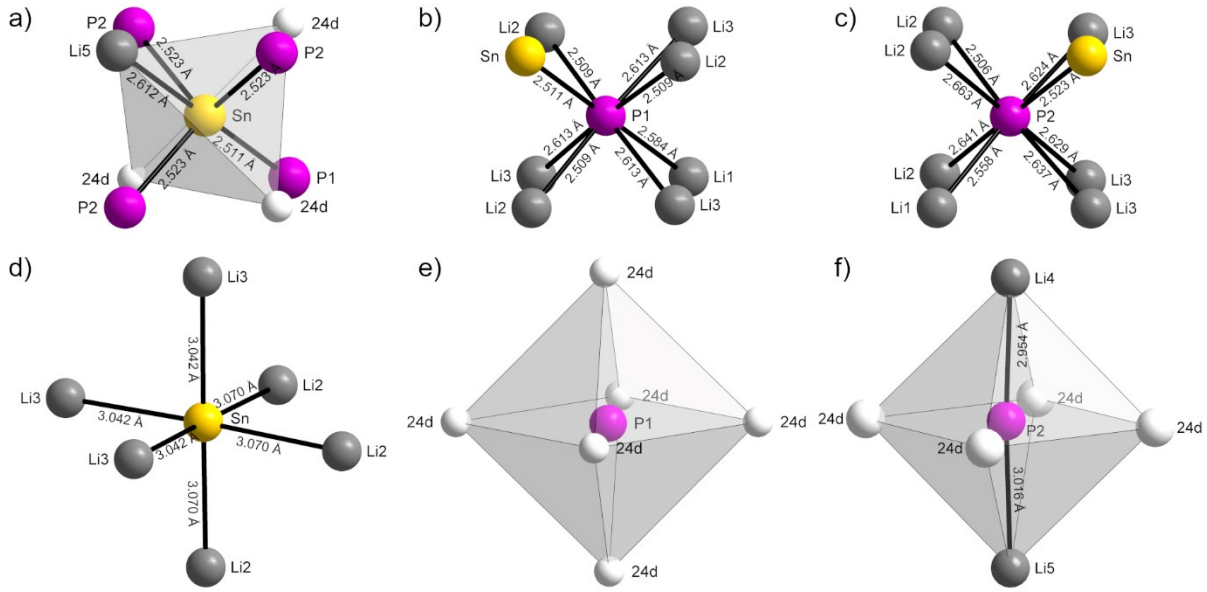

Figure S3. Coordination polyhedra of the atoms Sn, P1 and P2 in *α*-Li_8SnP_4. The nearest neighbors are arranged in a tetrahedral/cubic coordination (a-c), whereas the next nearest neighbors are arranged in an octahedral arrangement (d-f). Unoccupied sites are indicated by white spheres.

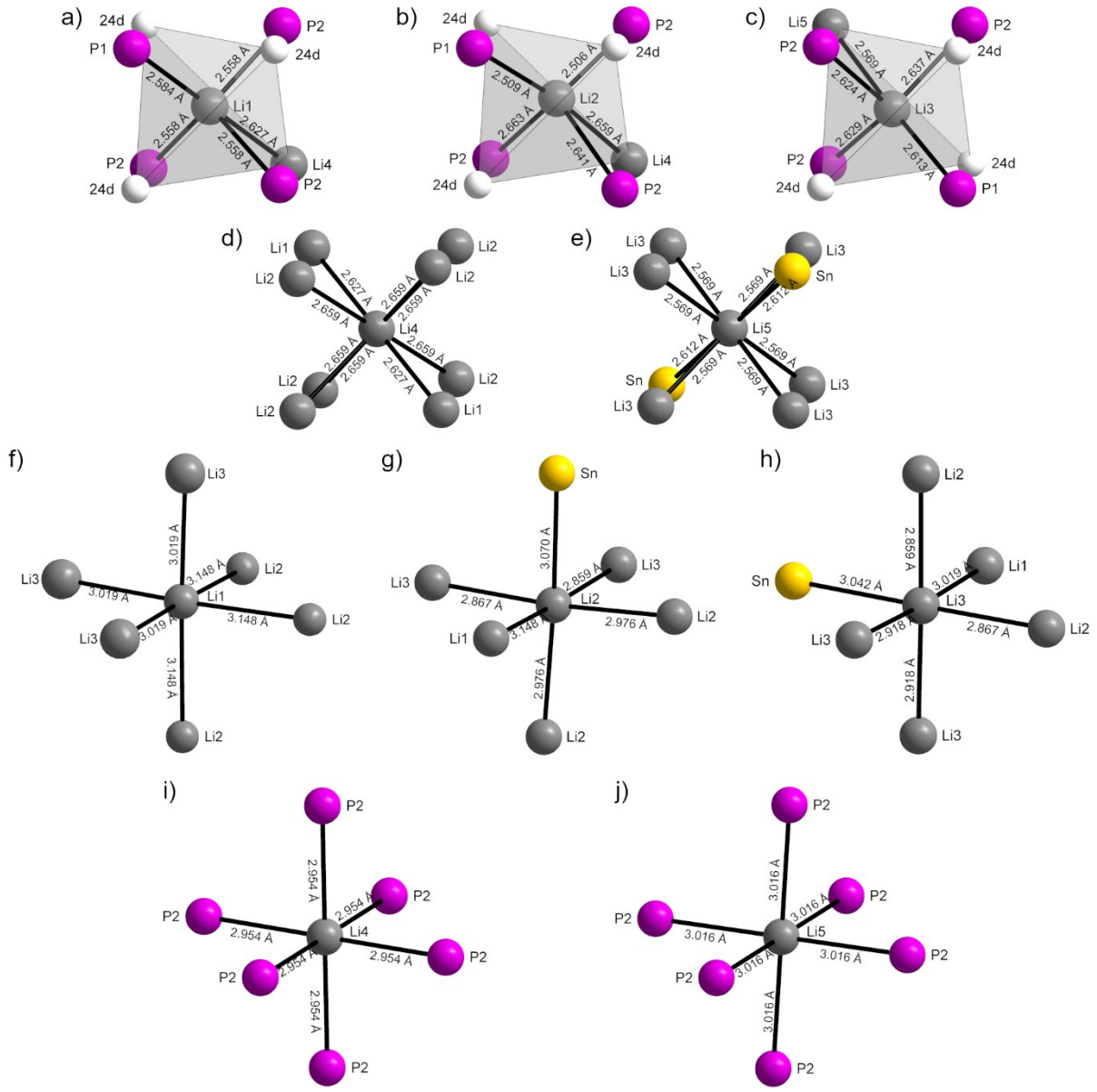

Figure S4. Coordination polyhedra of the atoms Li1-Li5 in α-Li_8SnP_4. The nearest neighbors are arranged in a tetrahedral/cubic coordination (a-e), whereas the next nearest neighbors are arranged in an octahedral arrangement (f-j). Unoccupied sites are indicated by white spheres.

In β-Li_8SnP_4 the atoms Sn1 and Sn2 are surrounded by four atoms P1 and P2, respectively, in a tetrahedral coordination (Figure S5). Additionally, the atom Sn1 is tetrahedrally coordinated by four atoms Li6 with a probability of 50 %, whereas the atom Sn2 is tetrahedrally coordinated by four atoms Li7 with a probability of 16 %. The P atoms are centered in a slightly distorted cubic geometry consisting of one Sn and seven Li atoms (P1: 1×Sn1, 1×Li3, 3×Li4 and 3×Li5; P2: 1×Sn2, 1×Li1, 1×Li2, 1×Li3, 1×Li4 and 3×Li5).

In the next nearest coordination sphere the Sn atoms are surrounded by six Li atoms in a slightly distorted octahedral geometry (Sn1: 6×Li4; Sn2: 2×Li1 and 4×Li5). Moreover, the atom P1 is surrounded by three atoms Li6 and Li7, each with the corresponding probability. The second coordination sphere of the atom P2 contains only one atom Li6 and five atoms Li7.

Finally, the coordination polyhedra of the atoms Li1-Li7 are shown (Figure S6) as a guide to the eye evaluating the rather complex diffusion pathways (one-particle potential) resulting from the distortion of the P lattice. Due to this, the single connections of the tetrahedral and octahedral voids are visible simplifying the comprehension of the obtained results based on nuclear density maps from powder neutron diffraction experiments at 1000 K.

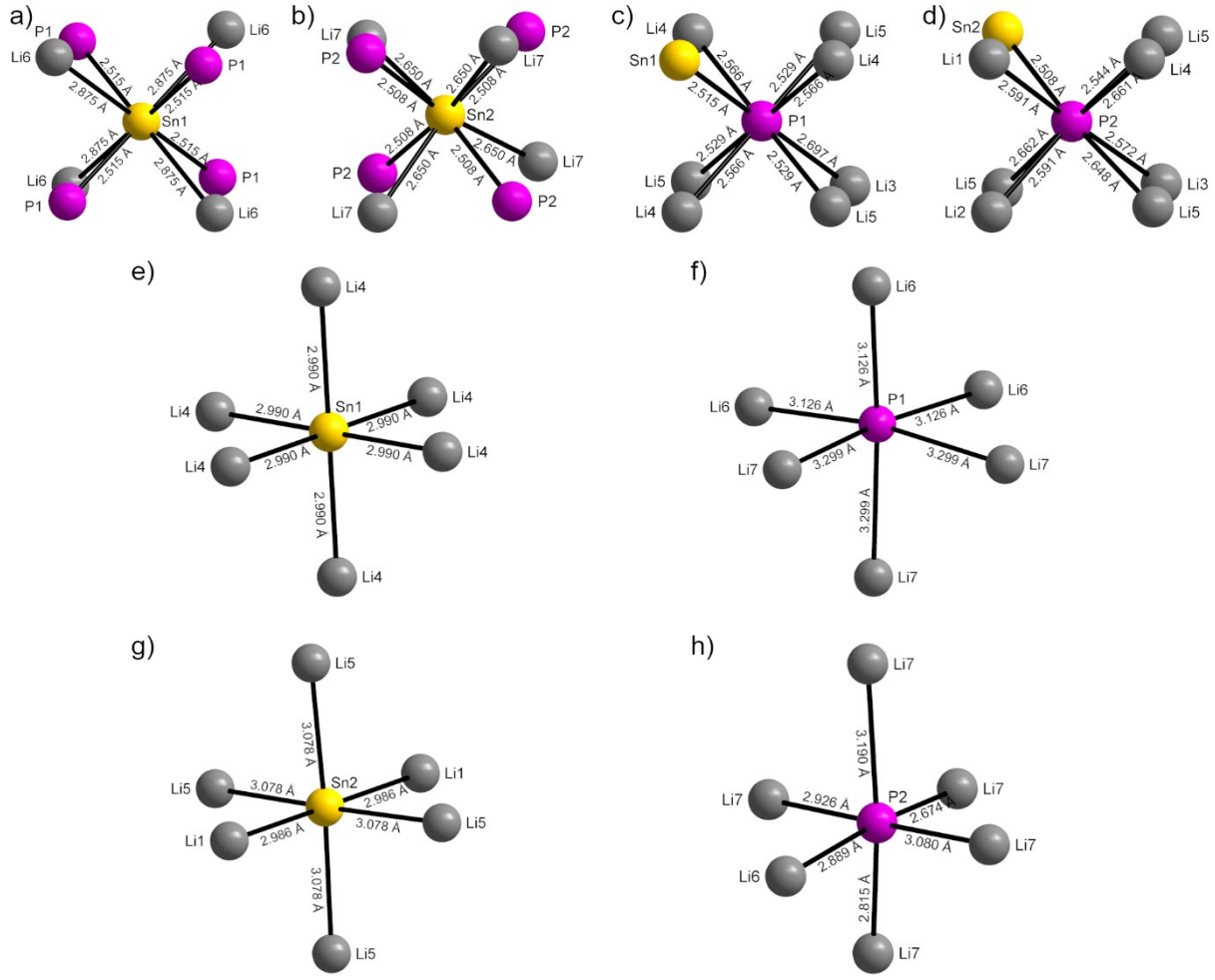

Figure S5. Coordination polyhedra of the atoms Sn1, Sn2, P1, and P2 in β-Li_8SnP_4. The nearest neighbors are arranged in a tetrahedral/cubic coordination (a-d), whereas the next nearest neighbors are arranged in an octahedral arrangement (e-h).

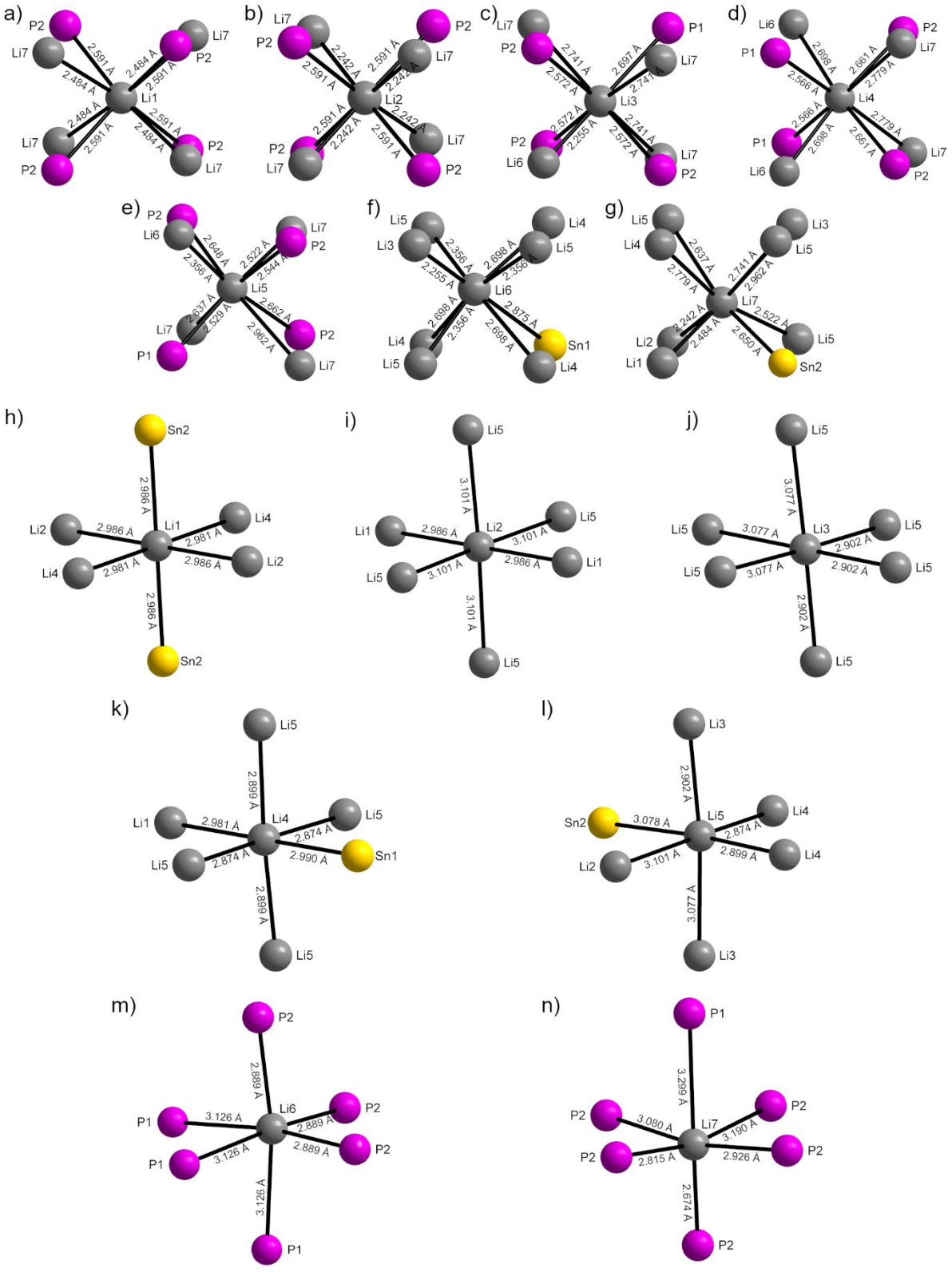

Figure S6. Coordination polyhedra of the atoms Li1-Li7 in β-Li_8SnP_4. The nearest neighbors are arranged in a tetrahedral/cubic coordination (a-g), whereas the next nearest neighbors are arranged in an octahedral arrangement (h-n).

Differential Scanning Calorimetry (DSC) and Phase Transition Experiments

DSC analyses were carried out from room temperature to 1023 K, staring from the reactive mixture "Li_8SnP_4" as well as from crystalline samples of α- and β-Li_8SnP_4, respectively. The recorded thermograms show very weak and indistinct thermal effects in the range between 780 to 840 K indicating the phase transition between the two modifications (Figure S7). The relatively small signals show only minor differences in terms of energy gain or loss.

Comparing the data with the powder X-ray diffraction experiments carried out after the DSC measurements identifies the β-phase as the more stable modification as it is the only phase present in all three samples (Figure S8). Thus, the thermal effect at about 800 K indicates the (delayed) formation of α-Li_8SnP_4, whereas the second thermal effect at about 830 K shows the phase transition starting from the α-modification into β-Li_8SnP_4, which is stable during cooling. As an exception, the thermogram of the reactive mixture shows a tiny thermal effect (at 780 K) during the first cooling cycle indicating a (partial) phase transition from β-Li_8SnP_4 (formed during heating) to the α-modification. In the second cycle, the latter compound finally converts completely into the β-phase (at 828 K), and, since there is no further signal observed during cooling, the diffraction pattern shows phase-pure β-Li_8SnP_4.

For a better understanding of the phase transition process high-temperature experiments have been carried out, revealing a fast and thus complete transition of α-Li_8SnP_4 to β-Li_8SnP_4 upon heating to 773 K. This was also observed during the temperature-dependent powder neutron diffraction measurements. By contrast, the phase transition from β- to α-Li_8SnP_4 takes much longer since a mixture of both modifications is obtained by powder X-ray diffraction experiments after an annealing time of 72 h at 673 K (Figure S9). These findings additionally confirm the results from DSC measurements mentioned above.

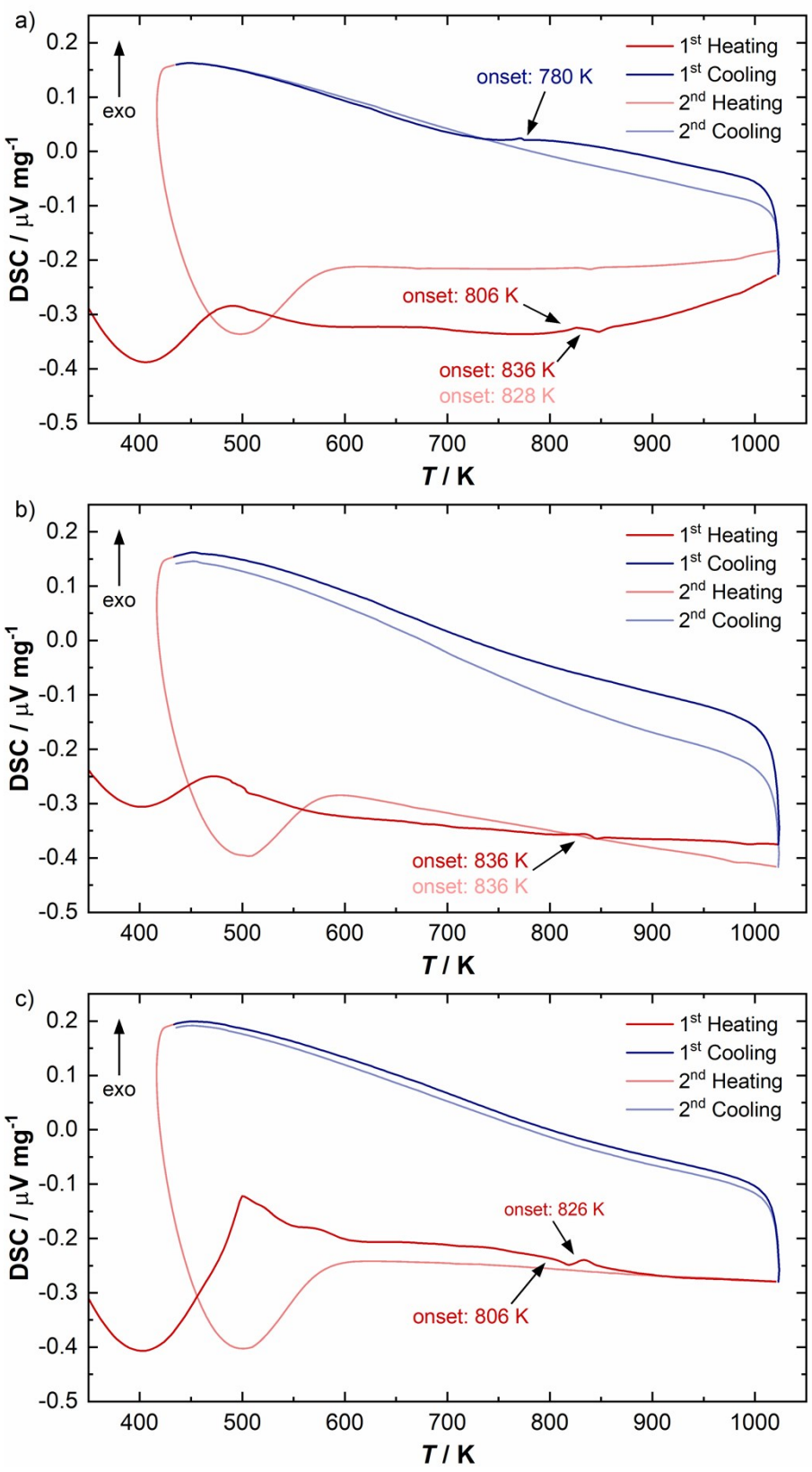

Figure S7. a) DSC thermogram of the reactive mixture "Li_8SnP_4". b) DSC thermogram of α-Li_8SnP_4. c) DSC thermogram of β-Li_8SnP_4. The arrows and numbers indicate the onset temperatures of the corresponding thermal effects.

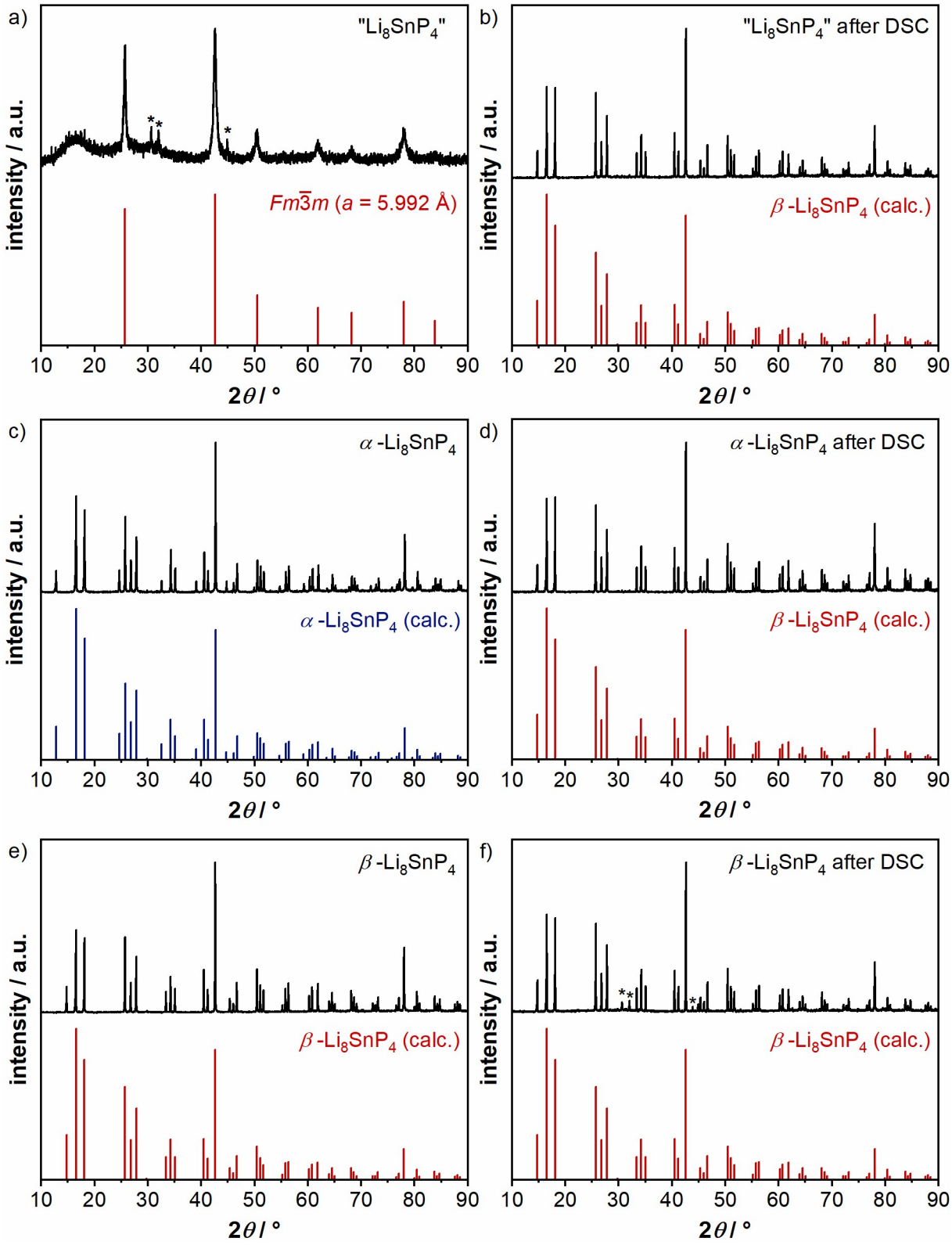

Figure S8. a, b) Powder X-ray diffractogram of the reactive mixture "Li_8SnP_4" before and after DSC measurement. c, d) Powder X-ray diffractogram of α-Li_8SnP_4 before and after DSC measurement. e, f) Powder X-ray diffractogram of β-Li_8SnP_4 before and after DSC measurement. The calculated diffraction pattern of α- and β-Li_8SnP_4 are shown in blue and red, respectively, and β-Sn is indicated by *.

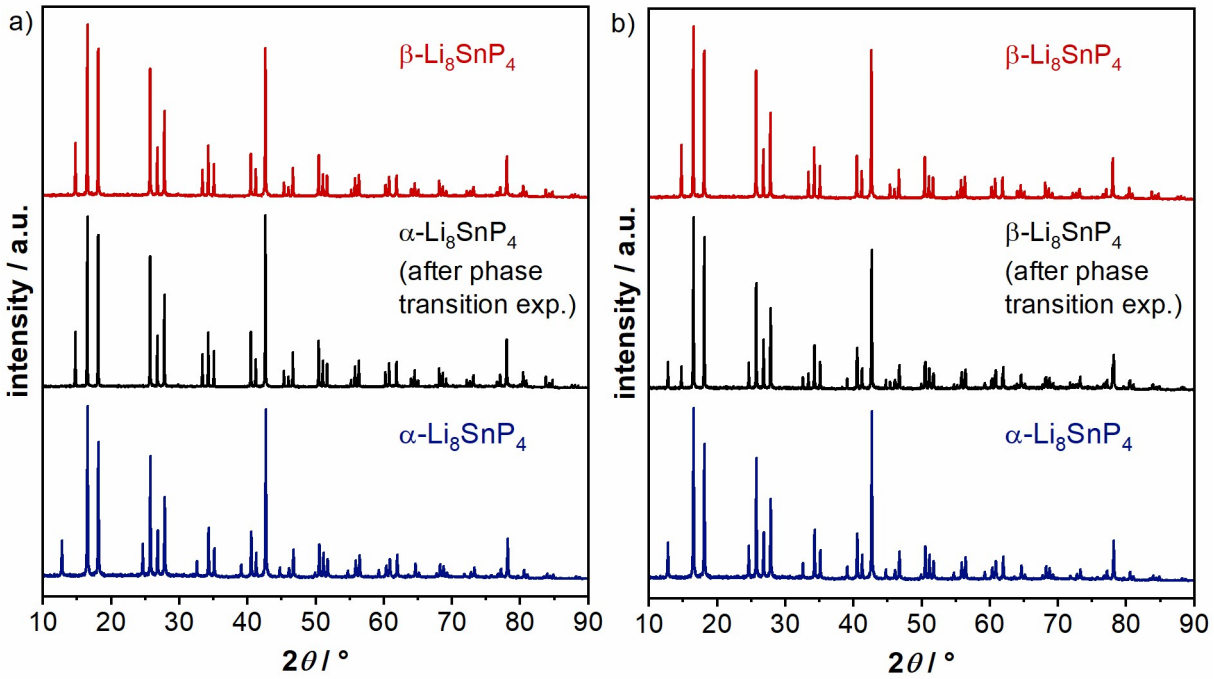

Figure S9. a) Powder X-ray diffractogram of α-Li_8SnP_4 after the phase transition experiment (black). b) Powder X-ray diffractogram of β-Li_8SnP_4 after the phase transition experiment (black). For better comparison the powder X-ray diffractogram of α- and β-Li_8SnP_4 (before the phase transition experiment) are additionally shown in blue and red, respectively.

^{6}Li, ^{119}Sn and ^{31}P MAS NMR Spectroscopy

^{6}Li MAS NMR spectra of α- and β-Li_8SnP_4

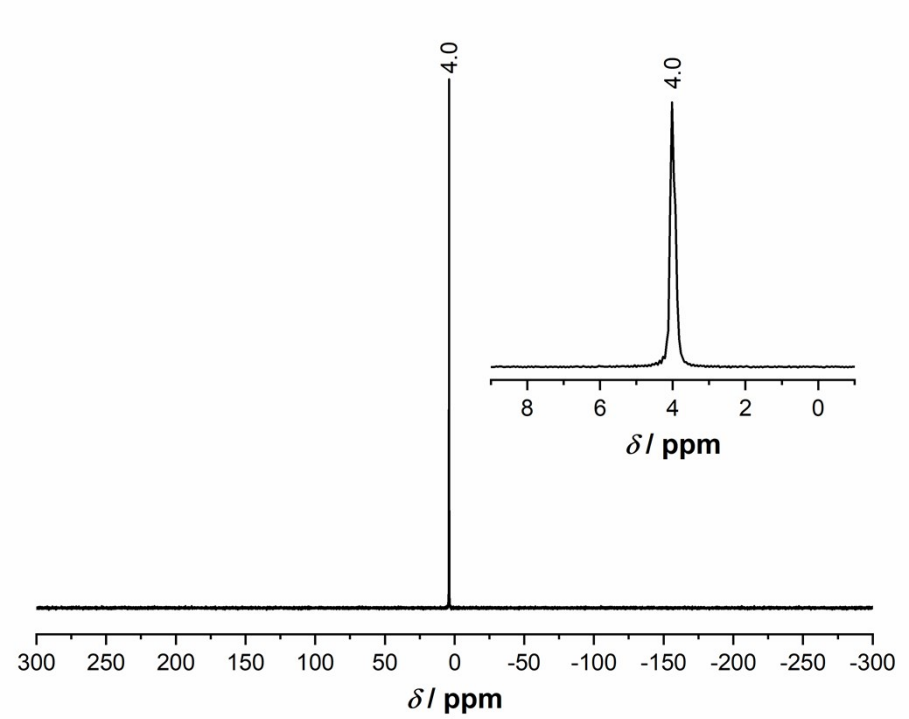

Figure S10. ^{6}Li MAS NMR spectrum of α-Li_8SnP_4. The inset shows the proximity of the signal and its shape.

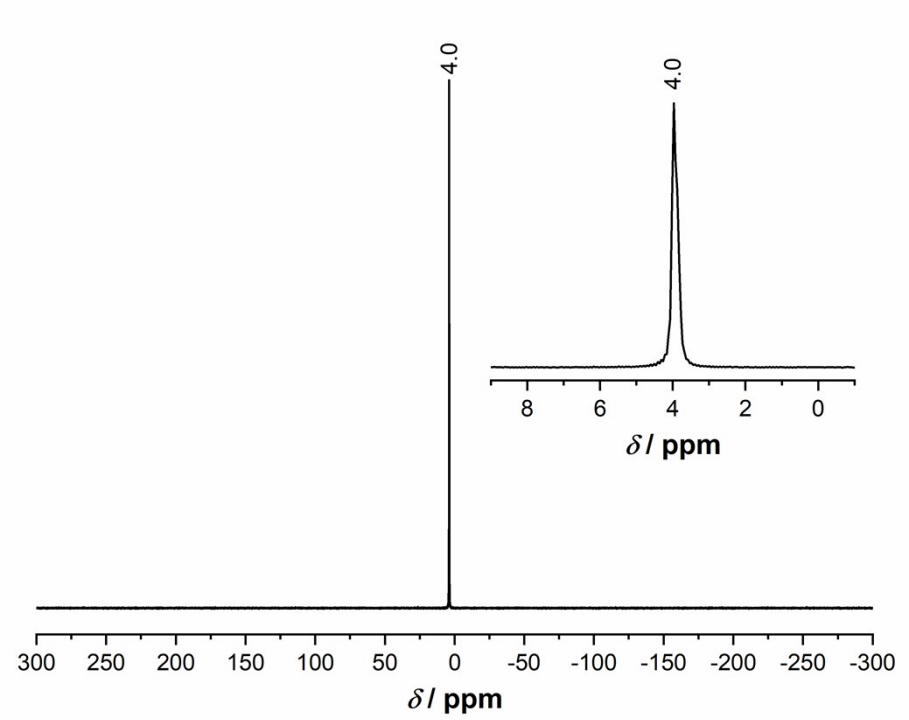

Figure S11. ^{6}Li MAS NMR spectrum of β-Li_8SnP_4. The inset shows the proximity of the signal and its shape.

^{31}P MAS NMR spectra of α- and β-Li_8SnP_4

For an evaluation of the ^{31}P spectra of α- and β-Li_8SnP_4 in greater detail the observed signals and their integrals were analyzed using the peak-fitting function implemented in the OriginPro 2020 software.[1] All signals were fitted applying the Lorentzian peak type.

The ^{31}P NMR spectra of α-Li_8SnP_4 and β-Li_8SnP_4 show several resonances in the range between −240 and −270 ppm (Figures S12a and S13a). Deconvolution of the overlapping signals revealed four resonances, two singlets (s_1 and s_2) and two doublets (d_1 and d_2) with slightly different coupling constants, in both spectra (Figures 12b and 13b and Tables S20 and S23).

In case of β-Li_8SnP_4 the deconvolution of the two overlapping signals at about −253.8 ppm was unfeasible. However, the sum of the integrated intensity of the signal at −243.5 and −263.8 ppm is nearly equal to the integrated intensity of the overlapping signals at −253.8 ppm.

More detailed evaluation of the data exhibits identical chemical shifts for one singlet and one doublet, each (singlet-doublet-pairs s_1d_1 and s_2d_2). The ratio of the total integrated intensities of the two singlet-doublet-pairs is 1:3 (Tables S21 and S24) corresponding to the multiplicity of the atoms P1 and P2 (8*c* and 24*d* for α-Li_8SnP_4 and 8*e* and 24*i* for β-Li_8SnP_4). The implementation of the deconvolution and evaluation of the integrated intensities exemplifies the correlation between the intensity ratios of a singlet-doublet-pair and the ratio of the natural abundance of NMR-active and -inactive Sn nuclides (Tables S22, S25 and S26). However, deviations from the expected values — especially in case of the natural abundance ratio — are strongly correlated with the results obtained *via* deconvolution as the signals are strongly superimposed. Here, in particular the results concerning signals with relative intensities < 10 % show large errors when extrapolated to the natural abundance, demonstrating the limits of this approach.

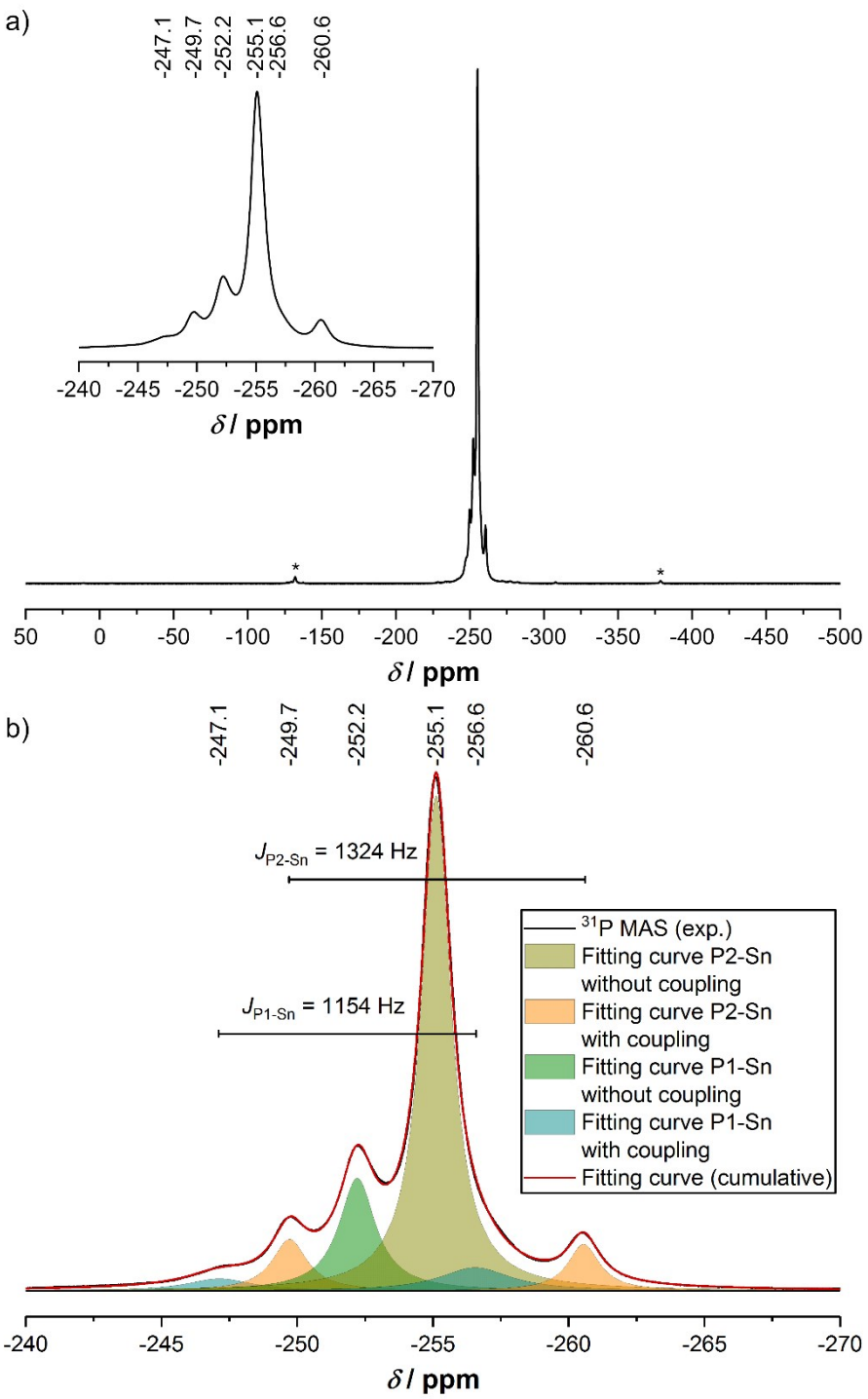

Figure S12. a) ^{31}P MAS NMR spectrum of α-Li_8SnP_4 (15 kHz). Spinning sidebands indicated by *. The inset shows the proximity of the signal and its shape. b) Deconvolution of the obtained signals. Fitting of the overlapping signals between −270 and −240 ppm (red) results in two singlets (olive and green) and two doublets (orange and blue).

Table S20. Details of the fitted peak area of the deconvolution of singlet 1 (s_1, olive), singlet 2 (s_2, green), doublet 1 (d_1, orange), and doublet 2 (d_2, blue) of the ^{31}P MAS NMR spectrum of α-Li_8SnP_4 (Figure S12b).

α-Li_8SnP_4	d_2	d_1	s_2	s_1	d_2	d_1
overall fit	3.1 %	7.3 %	16.8 %	60.1 %	6.5 %	6.1 %
fit s_1	---	---	---	100 %	---	---
fit s_2	---	---	100 %	---	---	---
fit d_1	32.3 %	---	---	---	67.7 %	---
fit d_2	---	54.5 %	---	---	---	45.5 %
ratio	0.65	1.09	1.00	1.00	1.35	0.91

Table S21. Comparison of the singlet-doublet-pair 1 (s_1d_1, yellow) and the singlet-doublet-pair 2 (s_2d_2, teal) of the ^{31}P MAS NMR spectrum of α-Li_8SnP_4 (Figure S12b).

α-Li_8SnP_4	s_1	d_1	s_2	d_2
overall fit	60.1 %	13.4 %	16.8 %	9.6 %
fit s_1d_1	73.5 %		---	
fit s_2d_2	---		26.4%	
Ratio	2.94		1.06	

Table S22. Comparison of the corresponding singlet-doublet-pairs of the ^{31}P MAS NMR spectrum of α-Li_8SnP_4 (Figure S12b) with the natural abundance of NMR active Sn nuclides (^{115}Sn, ^{117}Sn, and ^{119}Sn) and NMR inactive Sn nuclides, respectively (Table S26).

α-Li_8SnP_4	s_1	d_1	s_2	d_2
s vs. d	81.8 %	18.2 %	63.6 %	36.4 %
Active	---	16.6 %	---	16.6 %
Inactive	83.4 %	---	83.4 %	---
Deviation	−1.6 %	+1.6 %	−19.8 %	+19.8 %

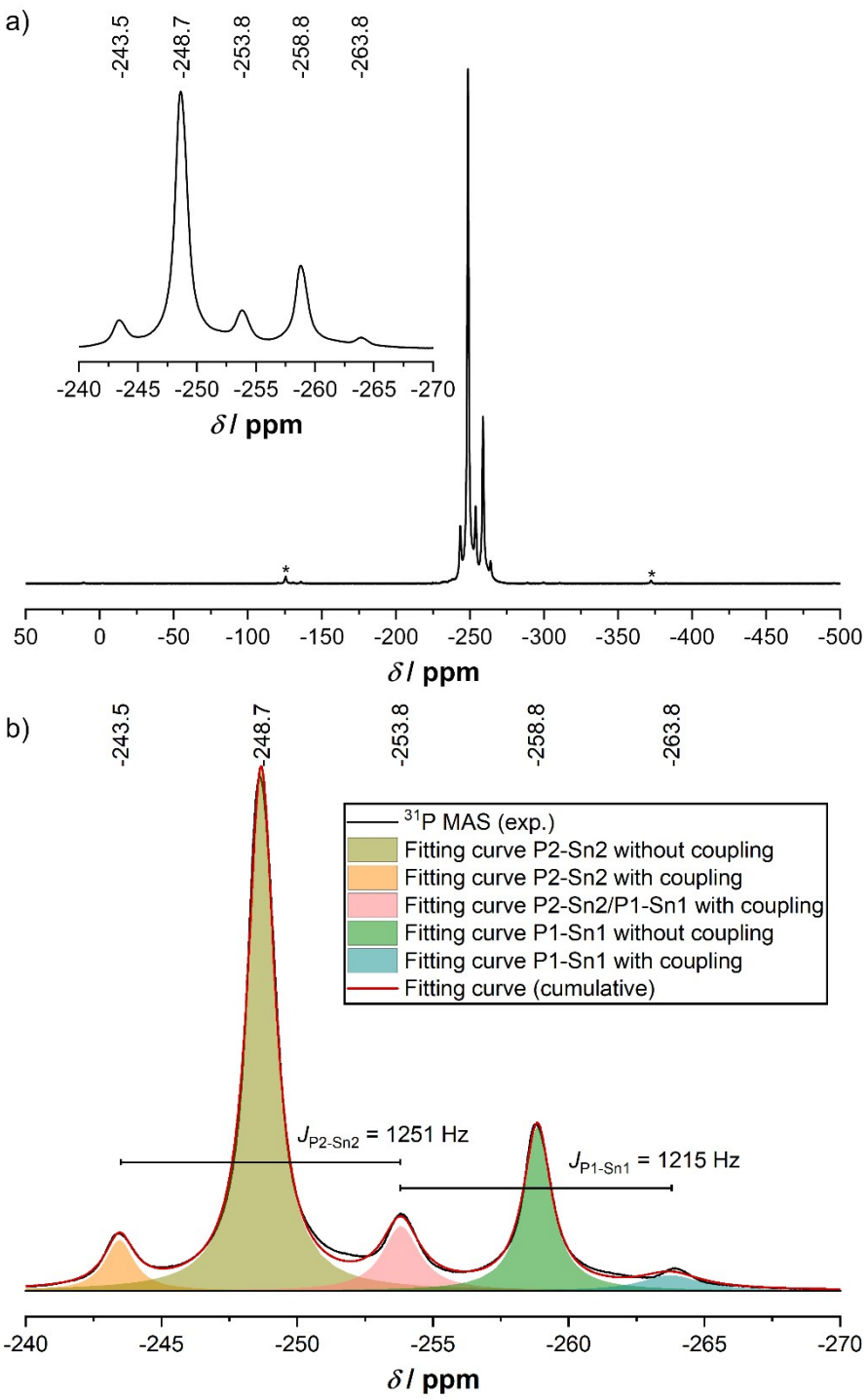

Figure S13. a) ^{31}P MAS NMR spectrum of β-Li_8SnP_4 (15 kHz). Spinning sidebands indicated by *. The inset shows the proximity of the signal and its shape. b) Deconvolution of the obtained signals. Fitting of the overlapping signals between −270 and −240 ppm (red) results in two singlets (olive and green) and two doublets (orange and blue). The pink area results from overlapping of the orange and the blue signal. Here a deconvolution was not possible.

Table S23. Details on the fitted peak area of the deconvolution of singlet 1 (s_1, olive), singlet 2 (s_2, green), doublet 1 (d_1, orange) and doublet 2 (d_2, blue) of the ^{31}P MAS NMR spectrum of β-Li_8SnP_4 (Figure S13b). The overlapping areas of d_1 and d_2, which failed the deconvolution are shown in pink (d_{1+2}). Approximated values are marked by "~".

β-Li_8SnP_4	d_1	s_1	d_{1+2}		s_2	d_2
overall fit	6.1 %	60.3 %	10.2 %		19.6 %	3.8 %
fit s_1	---	100 %	---		---	---
fit s_2	---	---	---		100 %	---
fit d_1	~50 %	---	~50 %	---	---	---
fit d_2	---	---	---	~50 %	---	~50 %
ratio	1.00	1.00	1.00	1.00	1.00	1.00

Table S24. Comparison of the singlet-doublet-pair 1 (s_1d_1, yellow) and the singlet-doublet-pair 2 (s_2d_2, teal) of the ^{31}P MAS NMR spectrum of β-Li_8SnP_4 (Figure S13b). Approximated values are marked by "~".

β-Li_8SnP_4	s_1	d_1	s_2	d_2
overall fit	60.3 %	~12.2 %	19.6 %	~7.6 %
fit s_1d_1	~72.5 %		---	
fit s_2d_2	---		~27.2 %	
Ratio	~2.9		~1.1	

Table S25. Comparison of the corresponding singlet-doublet-pairs of the ^{31}P MAS NMR spectrum of β-Li_8SnP_4 (Figure S13b) with the natural abundance of NMR active Sn nuclides (^{115}Sn, ^{117}Sn, and ^{119}Sn) and NMR inactive Sn nuclides, respectively (Table S26).

β-Li_8SnP_4	s_1	d_1	s_2	d_2
s vs. d	83.2 %	16.8 %	72.1 %	27.9 %
Active	---	16.6 %	---	16.6 %
Inactive	83.4 %	---	83.4 %	---
Deviation	−0.2 %	+0.2 %	−11.3 %	+11.3 %

Table S26. Nuclear spin and natural abundance of Sn isotopes.

Isotopes	Spin[2]	Abundance[3]
^{112}Sn	$I = 0$	0.97(1) %
^{114}Sn	$I = 0$	0.66(1) %
^{115}Sn	$I = 1/2$	0.34(1) %
^{116}Sn	$I = 0$	14.54(9) %
^{117}Sn	$I = 1/2$	7.68(7) %
^{118}Sn	$I = 0$	24.22(9) %
^{119}Sn	$I = 1/2$	8.59(4) %
^{120}Sn	$I = 0$	32.58(9) %
^{122}Sn	$I = 0$	4.63(3) %
^{124}Sn	$I = 0$	5.79(5) %

^{119}Sn MAS NMR spectra of α- and β-Li_8SnP_4

In order to distinguish the different signals and their integrals the ^{119}Sn spectra of α- and β-Li_8SnP_4 were evaluated in greater detail using the peak-fitting-function implemented in the OriginPro 2020 software.[1] All signals were fitted applying the Lorentzian peak type.

In the ^{119}Sn NMR spectra of α-Li_8SnP_4 and β-Li_8SnP_4 several signals are observed in the range between 150 and 70 ppm (Figures S14a and S15a). Deconvolution of the partially overlapping signals unveiled a quartet of doublets with two slightly different coupling constants for α-Li_8SnP_4 (Figure S14b) and two quintets with an integrated intensity ratio of 1:3 for β-Li_8SnP_4 (Figure S15b). The splitting trees as well as the integrated intensities obtained by deconvolution of the multiplets are shown in Figure S16 as well as in Tables S27 and S28, respectively.

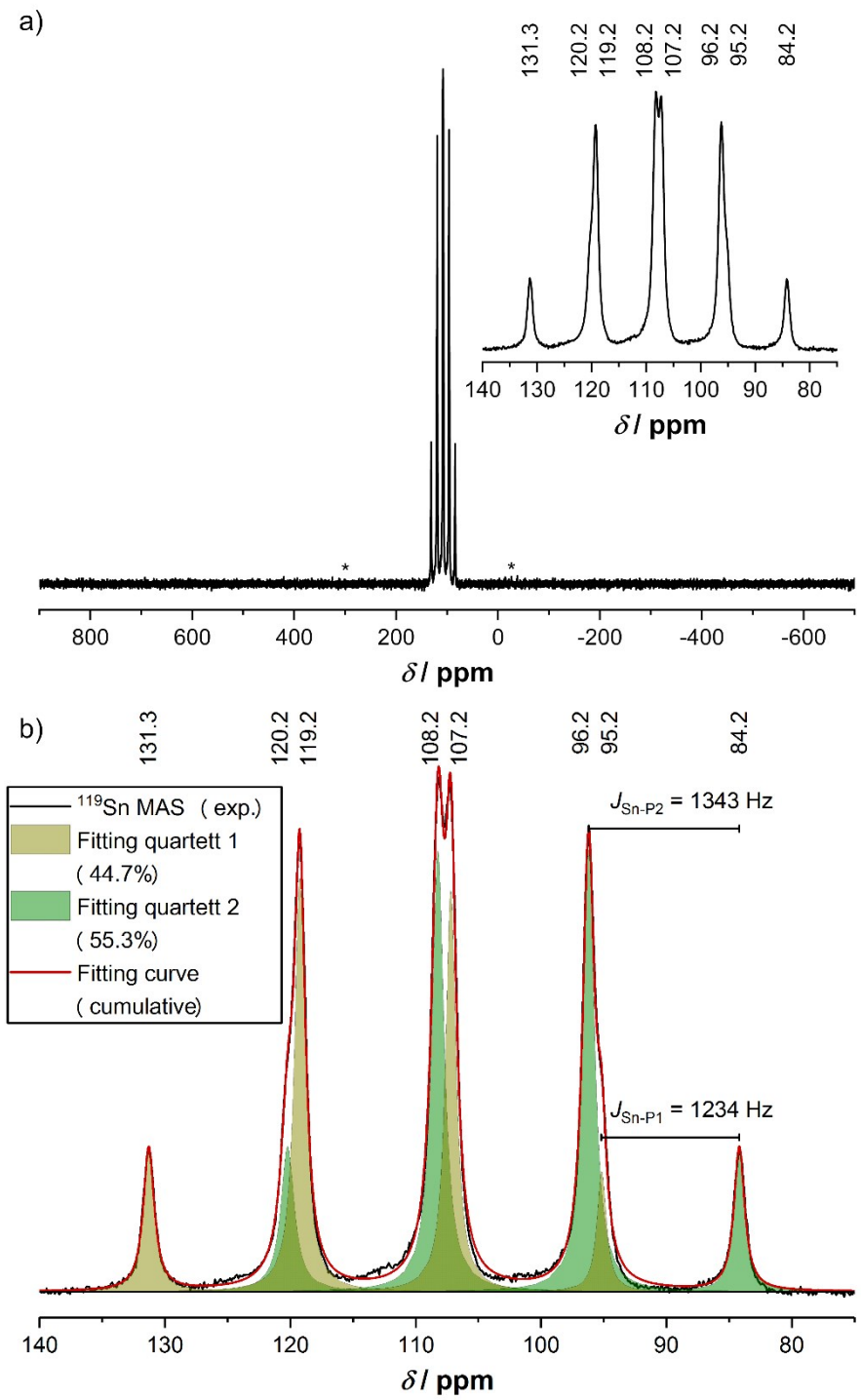

Figure S14. a) ^{119}Sn MAS NMR spectrum of α-Li_8SnP_4 (15 kHz). Spinning sidebands indicated by *. The inset shows the proximity of the signal and its shape. b) Deconvolution of the signals. Fitting of the overlapping signals between 70 and 140 ppm (red) results in a doublet of quartets (olive and green).

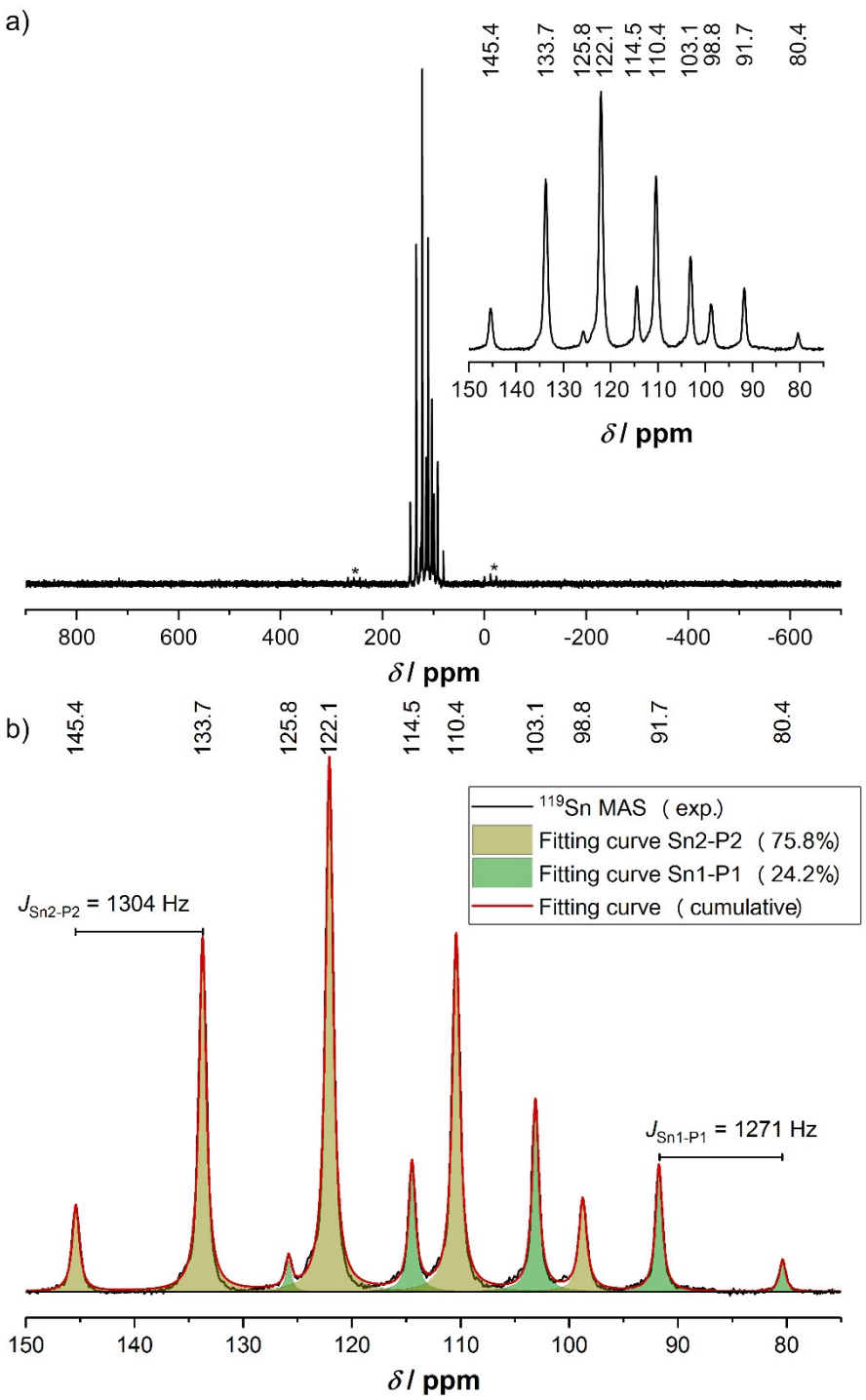

Figure S15. a) ^{119}Sn MAS NMR spectrum of β-Li_8SnP_4 (15 kHz). Spinning sidebands indicated by *. The inset shows the proximity of the signal and its shape. b) Deconvolution of the obtained signals. Fitting of the overlapping signals between 70 and 150 ppm (red) results in two quintets (olive and green).

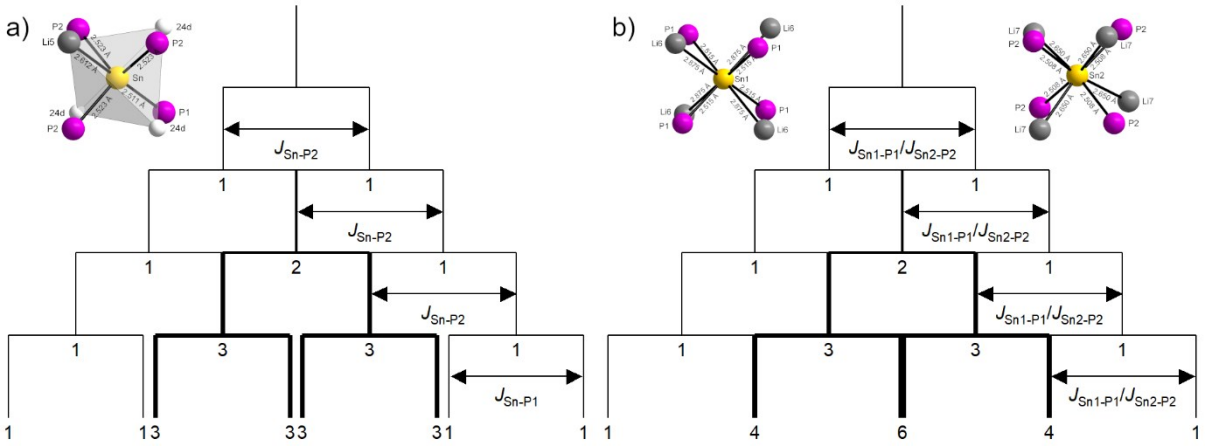

Figure S16. a) *J*-*J*-coupling of Sn with P1 (1234 Hz) and P2 (1343 Hz) in the ^{119}Sn NMR spectrum of α-Li_8SnP_4 resulting in a doublet of quartets. b) *J*-*J*-coupling of Sn1 with P1 (1271) and Sn2 with P2 (1304 Hz) in the ^{119}Sn NMR spectrum of β-Li_8SnP_4.

Table S27. Details of the deconvolution of quartet 1 (q_1, olive) and quartet 2 (q_2, green) of the ^{119}Sn MAS NMR spectrum of α-Li_8SnP_4 (Figure S14b). The ratio of the signals is normalized to 1/16 = 0.0625 or 6.25 %.

α-Li_8SnP_4	q_1	q_2	q_1	q_2	q_1	q_2	q_1	q_2
overall fit	6.1 %	7.8 %	17.5 %	21.2 %	16.5 %	20.4 %	4.5 %	5.9 %
ratio	0.98	1.25	2.80	3.39	2.64	3.26	0.72	0.94

Table S28. Details of the deconvolution of quintet 1 ($quint_1$, olive) and quintet 2 ($quint_2$, green) of the ^{119}Sn MAS NMR spectrum of β-Li_8SnP_4 (Figure S15b). The ratio of the signals is normalized to 1/16 = 0.0625 or 6.25 %.

β-Li_8SnP_4	quint 1	quint 1	quint 2	quint 1	quint 2	quint 1	quint 2	quint 1	quint 2	quint 2
overall fit	4.3 %	18.5 %	1.2 %	28.5 %	6.1 %	19.5 %	9.4 %	5.1 %	6.1 %	1.4 %
fit $quint_1$	5.7 %	24.4 %	---	37.6 %	---	25.7 %	---	6.7 %	---	---
fit $quint_2$	---	---	5.0 %	---	25.2 %	---	38.8 %	---	25.2 %	5.7 %
ratio	0.91	3.90	0.80	6.02	4.03	4.11	6.21	1.07	4.03	0.91

Electrochemical Impedance Spectroscopy (EIS)

For the determination of E_A^{PEIS} temperature-dependent PEIS measurements were carried out. Figure S17 shows one selected spectrum of each temperature for both modifications.

The impedance spectra of Li_8SiP_4, and α- and β-Li_8SnP_4 at 299 K are depicted in Figure S18.

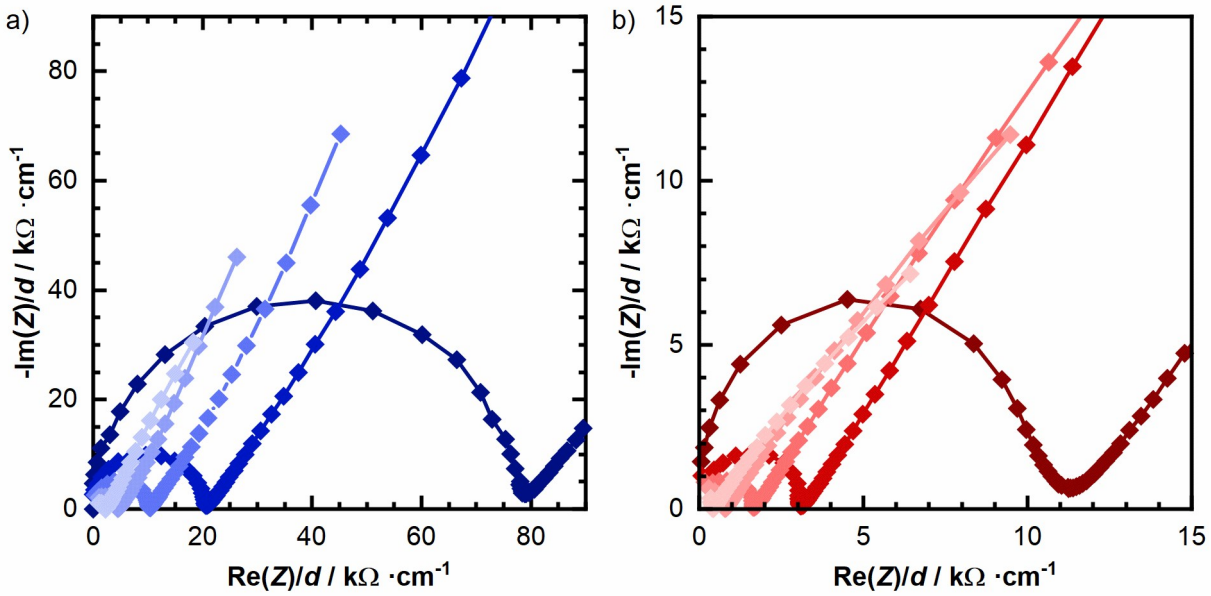

Figure S17. Nyquist plots of α- and β-Li_8SnP_4, measured under blocking conditions at 273, 298, 313, 333, and 353 K and normalized to the pellet thickness. a) α-Li_8SnP_4 from 273 K (dark blue) to 353 K (light blue) b) β-Li_8SnP_4 from 273 K (dark red) to 353 K (light red).

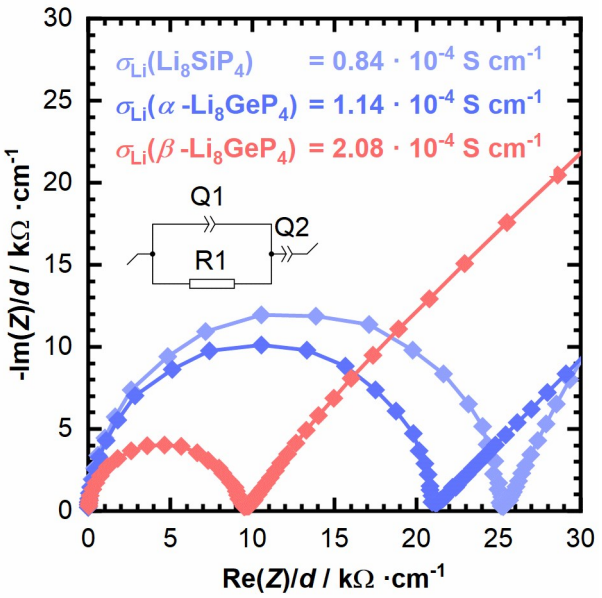

Figure S18. Nyquist plots of Li_8SiP_4 (light blue), α- and β-Li_8GeP_4 (blue and red), measured under blocking conditions at 299 ± 0.5 K and normalized to the pellet thickness. The equivalent circuit which was used for fitting is displayed in the inset.

References

1. OriginPro, Version 2020. Northampton, MA, USA: OriginLab Corporation; 2020.
2. W. Makulski, *J Mol Struct*, 2012, **1017,** 45-50.
3. IUPAC, *Pure Appl Chem*, 1998, **70,** 217-235.